John von Neumann Institute for Computing

NIC

Static and Time-Dependent Many-Body Effects via Density-Functional Theory

Heiko Appel, Eberhard K. U. Gross

Static and Time-Dependent Many-Body Effects via Density-Functional Theory

Heiko Appel and Eberhard K. U. Gross

Institut für Theoretische Physik, Freie Universität Berlin
Arnimallee 14, 14195 Berlin, Germany
E-mail: {appel, hardy}@physik.fu-berlin.de

After introducing the basic concepts of static and time-dependent density-functional theory we focus on numerical algorithms for the propagation of the time-dependent Kohn-Sham equations. Two different methods, based on modifications of the Crank-Nicholson and the split-operator propagation schemes, respectively, are presented. We discuss some strategies for the parallelization of the Kohn-Sham propagation using state-of-the-art message-passing protocols. Finally, some results for atoms in strong laser fields are presented.

1 Introduction

The non-relativistic treatment of quantum-mechanical problems in solid-state physics or quantum chemistry requires, in principle, the solution of the full many-body Schrödinger equation for the combined system of electrons and nuclei

$$\left(\hat{H} - E\right)|\Psi\rangle = 0. \tag{1}$$

Here the Hamiltonian is given by

$$\hat{H} = \hat{T}_{\mathrm{n}} + \hat{W}_{nn} + \hat{V}_{\mathrm{ext},n} + \hat{T}_e + \hat{W}_{ee} + \hat{V}_{\mathrm{ext},e} + \hat{W}_{en}, \tag{2}$$

where $\hat{T}_n$, $\hat{T}_e$ denote the kinetic-energy operators of the nuclei and electrons, respectively, $\hat{W}_{nn}$, $\hat{W}_{ee}$ and $\hat{W}_{en}$ contain the interparticle Coulomb interactions, and $\hat{V}_{\mathrm{ext},n}$, $\hat{V}_{\mathrm{ext},e}$ represent the external potentials acting on the system. Using the solution of eq. (1) all observables of interest are readily evaluated from the corresponding expectation value

$$A = \langle\,\Psi\,|\,\hat{A}\,|\,\Psi\,\rangle. \tag{3}$$

While eq. (1) provides the correct starting point for the quantum mechanical treatment of any many-body system, its numerical solution becomes exceedingly difficult with increasing particle number. To see how this comes about even for relatively small finite systems consider, as an example, the nitrogen atom. Suppose that we want to store the values of the electronic ground-state wave function in a rough table containing only 10 entries for each Cartesian coordinate of the 7 electrons. This results in $10^{(7\times3)}$ entries for the table. Furthermore, reserving only one byte of memory per entry the data of the table will require 10^{11} DVD's for storage. Here we have assumed an ample capacity of 10^{10} bytes per DVD. Turning from finite to extended systems the situation becomes even worse. In the case of solids with particle numbers of the order of 10^{23} the task of solving eq. (1) becomes completely non-feasible. This simple example illustrates that, for sufficiently large systems, the direct numerical determination of the many-body wave function is neither possible nor desirable.

In the last decades density-functional theory (DFT) has become a very popular approach for the quantum-mechanical treatment of many-particle systems. Instead of using the complicated many-body wave function, traditional DFT deals with the electronic ground-state density

$$\rho(\mathbf{r}) = N \int d^3 r_2 \int d^3 r_3 \cdots \int d^3 r_N \, |\psi(\mathbf{r}, \mathbf{r_2}, \cdots, \mathbf{r_N})|^2 \tag{4}$$

as the basic variable. Within the framework of DFT it can be shown that all observables are functionals of the density only. The next section introduces briefly the basic notions of static and time-dependent DFT (TDDFT). Having provided the formal background for the discussion we then turn to numerical aspects of the propagation in section 3. We first review the well known Crank-Nicholson[1,2] and split-operator spectral method[3] and then introduce the modifications necessary for the propagation of the time-dependent Kohn-Sham equations. Section 3.3 is devoted to a discussion on the parallelization of the time-dependent Kohn-Sham equations. Finally, in section 4, we present some results for atoms in strong laser pulses.

2 Basic Concepts of DFT

2.1 Static Density Functional Theory

Traditional ground-state DFT[4,5] assumes the Born-Oppenheimer approximation, i.e., the nuclear motion is frozen and the nuclear centers are kept at fixed positions. The Coulomb interaction between the fixed nuclei and the electrons is described by an external potential $\hat{v}$ acting on the electrons only. Assuming this framework, the fundamental Hohenberg-Kohn theorem of density-functional theory can be summarized by the following three statements

(i) The external potential $\hat{v}$ (usually due to the nuclei) is uniquely determined by the electronic ground-state density. With the knowledge of $\hat{v}$ the complete electronic Hamiltonian, including the kinetic energy $\hat{T}_e$ and the Coulomb repulsion of the electrons $\hat{W}_{ee}$, is known

$$\hat{H} = \hat{T}_e + \hat{W}_{ee} + \hat{v} \,. \tag{5}$$

A formal solution of the many-body Schrödinger equation can then be used in principle to evaluate expectation values of any observable of interest. Hence, any observable of a static many-body system is a functional of its ground-state density.

(ii) Consider now a given system with a given (fixed) external potential $\hat{v}_0$. Then the total-energy functional

$$E_{v_0}[\rho] = \langle \, \psi[\rho] \, | \, \hat{T}_e + \hat{W}_{ee} + \hat{v}_0 \, | \, \psi[\rho] \, \rangle \tag{6}$$

obeys the Hohenberg-Kohn variational principle: The exact ground-state energy of the interacting electronic system is obtained if and only if the exact ground-state density ρ_0 is inserted in eq. (6). For densities ρ differing from ρ_0 the following inequality holds

$$E_0 = E_{v_0}[\rho_0] < E_{v_0}[\rho] \,. \tag{7}$$

Therefore, the ground-state energy E_0 and density ρ_0 can be determined by minimizing the functional $E_{v_0}[\rho]$. In practice this can be achieved by solving the Euler equation

$$\frac{\delta E_{v_0}[\rho]}{\delta\,\rho(\mathbf{r})} = 0 \,. \tag{8}$$

(iii) The density dependence of the functional $F[\rho]$

$$F[\rho] = \langle\,\psi[\rho]\,|\,\hat{T}_e + \hat{W}_{ee}\,|\,\psi[\rho]\,\rangle \tag{9}$$

is universal, i.e. it is the same for all systems with a fixed particle-particle interaction $\hat{W}_{ee}$.

For a proof of these statements the interested reader is referred to the literature[4,6]. Since the statements of the Hohenberg-Kohn theorem are independent of the specific form of the particle-particle interaction they hold in particular for the special case of noninteracting particles, where $\hat{W}_{ee} = 0$. This leads directly to the Kohn-Sham theorem:

Given the ground-state density $\rho(\mathbf{r})$ of an interacting system, the local, i.e., multiplicative single-particle potential $v_s[\rho]$ reproducing $\rho(\mathbf{r})$ as ground-state density of a non-interacting system is uniquely determined. Hence, $\rho(\mathbf{r})$ can be calculated from the effective single-particle equations (atomic units are used throughout)

$$\left(-\frac{\nabla^2}{2} + v_s[\rho](\mathbf{r}) - \epsilon_j\right)\varphi_j(\mathbf{r}) = 0, \qquad j = 1,..,N\,, \tag{10}$$

where the ground-state density ρ is obtained from the Kohn-Sham orbitals

$$\rho(\mathbf{r}) = \sum_{j=1}^{N} |\varphi_j(\mathbf{r})|^2 \,. \tag{11}$$

The Kohn-Sham eqns. (10) together with statement (i) of the Hohenberg-Kohn theorem provide an efficient practical scheme for the calculation of observables of static interacting-electron systems. In this way the solution of the full many-body Schrödinger equation can be circumvented: The Kohn-Sham equations are solved with some approximation for the functional $v_s[\rho]$, the density is calculated from the Kohn-Sham orbitals and finally the density is inserted in the corresponding functionals for the observables of interest.
Conventionally, the effective single-particle potential is decomposed in the following way

$$v_s[\rho](\mathbf{r}) = v_0(\mathbf{r}) + \int\frac{\rho(\mathbf{r}')}{|\mathbf{r}-\mathbf{r}'|}\,d^3r' + \frac{\delta E_{xc}[\rho]}{\delta\rho(\mathbf{r})}\,. \tag{12}$$

Here v_0 is the external potential, the second term describes the classical electrostatic interaction between the electrons and $v_{xc}(\mathbf{r}) = \delta E_{xc}[\rho]/\delta\rho(\mathbf{r})$ contains all exchange-correlation effects. Viewed historically, the most popular approximation for E_{xc} is the local-density approximation

$$E_{xc}[\rho] = \int\rho(\mathbf{r})\,e_{xc}^{\mathrm{unif}}(\rho(\mathbf{r}))\,d^3r\,. \tag{13}$$

Here $e_{xc}^{\text{unif}}(\rho)$ is the exchange-correlation energy per particle of the uniform electron gas with density ρ. The solution of the Kohn-Sham equations (10) involves a self-consistency cycle. From an initial guess for the orbitals, the density is calculated using (11). Inserting the density in (12) yields an approximation for the effective single-particle potential. In the next step the Kohn-Sham equations (10) are solved, resulting in a new set of orbitals. This cycle is repeated until self-consistency is reached.

Practical implementations of the Kohn-Sham equations follow different strategies. In quantum chemistry the Kohn-Sham orbitals are usually expanded in a basis set. This turns the effective single-particle equation into a simple eigenvalue problem. Typical choices for basis functions are Gaussian-type orbitals (GTO's) as implemented in GAUSSIAN 98[7] or Slater-type orbitals (STO's) as implemented in the Amsterdam density-functional program ADF[8]. For infinite periodic solids, the Kohn-Sham orbitals are Bloch functions. The latter can be expanded in plane waves (usually combined with a pseudopotential treatment of the core regions) as, e.g., in the FHI[9] code, in linearized augmented plane-waves (LAPW's) as in the WIEN2k[10] or the FLEUR[11] codes, in linear muffin-tin orbitals (LMTO's)[12] or in local orbitals as in the SIESTA[13] code.

2.2 Time-Dependent Density-Functional Theory

To describe interacting many-electron systems in time-dependent external fields an extension of the traditional ground-state theory is required. Recall that the ground-state theory establishes a one-to-one correspondence between ground-state densities and external potentials. In a time-dependent theory the question arises if there is also a one-to-one correspondence between time-dependent densities and time-dependent external potentials. The answer is positive and given by the Runge-Gross theorem[14,15], the time-dependent analogue of the Hohenberg-Kohn theorem:

> Two densities $\rho(\mathbf{r}, t)$ and $\rho'(\mathbf{r}, t)$ evolving from a common initial state $\Psi_0 = \Psi(t_0)$ under the influence of two potentials $v(\mathbf{r}, t)$ and $v'(\mathbf{r}, t)$ are always different provided that the potentials differ by more than a purely time-dependent function

$$v(\mathbf{r}, t) \neq v'(\mathbf{r}, t) + c(t). \tag{14}$$

The proof of this theorem assumes that the potentials $v(\mathbf{r}, t)$ and $v'(\mathbf{r}, t)$ are both Taylor expandable in the time coordinate around the initial time t_0.

Similar to the static case the one-to-one correspondence between time-dependent densities and time-dependent potentials can be established for arbitrary particle-particle interaction, in particular for a vanishing interaction. This ensures the uniqueness of a density-dependent single-particle potential $v_s(\mathbf{r}, t)$ which reproduces a given time-dependent density of an interacting system of interest. The time-dependent single-particle equations containing the effective potential $v_s(\mathbf{r}, t)$ are called the time-dependent Kohn-Sham (TDKS) equations

$$-i\partial_t \, \varphi_j(\mathbf{r}, t) = \left(-\frac{\nabla^2}{2} + v_s(\mathbf{r}, t)\right) \varphi_j(\mathbf{r}), \qquad j = 1, .., N \, . \tag{15}$$

Again the density is obtained from the orbitals

$$\rho(\mathbf{r}, t) = \sum_{j=1}^{N} |\varphi_j(\mathbf{r}, t)|^2 . \tag{16}$$

It is customary to partition the effective time-dependent potential as

$$v_s[\rho](\mathbf{r}, t) = v_0(\mathbf{r}, t) + \int \frac{\rho(\mathbf{r}', t)}{|\mathbf{r} - \mathbf{r}'|} d^3 r' + v_{xc}[\rho](\mathbf{r}, t) . \tag{17}$$

The second term on the right is the time-dependent Hartree potential and $v_{xc}[\rho](\mathbf{r}, t)$ is the time-dependent exchange-correlation potential. The simplest approximation possible for $v_{xc}[\rho](\mathbf{r}, t)$ is the adiabatic local-density approximation

$$v_{xc}[\rho](\mathbf{r}, t)^{\mathrm{ALDA}} = \left. \frac{d}{dn} e_{xc}^{\mathrm{unif}}(\rho) \right|_{\rho=\rho(\mathbf{r}, t)} . \tag{18}$$

From the way of its construction it can be seen directly that this approximation is local, both in space and time. More sophisticated approximations such as the optimized-effective potential have been suggested[16] which are non-local in space and time.

3 Propagation Methods for the TDKS Equations

Mathematically the solution of the time-dependent Kohn-Sham equations is an initial value problem. A given set of initial orbitals $\varphi_j(t_0)$ is propagated forward in time. No self-consistent iterations are required as in the static case. In terms of the time-evolution operator the orbitals at $t > t_0$ can be expressed as

$$\varphi_j(t) = \hat{U}(t, t_0)\varphi_j(t_0) \qquad j = 1, .., N , \tag{19}$$

where

$$\hat{U}(t, t_0) = \hat{T} \exp \left(-i \int_{t_0}^{t} \hat{H}_{KS}(\tau) d\tau \right) . \tag{20}$$

Note that due to the Hartree and exchange-correlation contributions the Kohn-Sham Hamiltonian is explicitly time-dependent even in the absence of a time-dependent external field. Because of this explicit dependence we have to keep the time-ordered exponential in the time-evolution operator.

The numerical task is now to find a discretized form of eq. (19). First of all let us consider the spatial representation of the orbitals. There are several discretizations possible:

- The values of the orbital are sampled on a 3D uniform Cartesian grid

$$\begin{aligned} \varphi_j(\mathbf{r}, t) &= \varphi_j(x, y, z, t) \\ &\rightarrow \varphi_j(x_k, y_l, z_m, t_n) , \end{aligned} \tag{21}$$

where

$$x_k = x_0 + k \, \Delta x, \qquad k_{\mathrm{min}} < k < k_{\mathrm{max}} , \tag{22}$$

y_l and z_m are treated similarly and

$$t_n = n \, \Delta t, \qquad n = 0, .., n_{\mathrm{max}} . \tag{23}$$

This is the most flexible but also the computationally most expensive approach.

- If the applied external field has certain symmetries, such as a laser field linearly polarized along the z-direction, a representation in cylindrical coordinates can be advantageous. In the case of linearly polarized lasers the angular quantum number m of the orbitals is preserved so that a possible representation of the orbitals is

$$\varphi_j(\mathbf{r},t) = \xi(\rho,z,t)\,e^{im\phi}\,. \tag{24}$$

  In this case the variables ρ, z and t are discretized.

- Another frequently used approach employs spherical coordinates. Here the orbital is expanded in spherical harmonics and only the radial functions are treated on a uniform grid

$$\varphi_j(\mathbf{r},t) = \sum_{l=0}^{L}\sum_{m=-l}^{l} R_{lm}(r,t)\,Y_l^m(\theta,\phi)\,. \tag{25}$$

Adaptive grids are also possible, require however a better bookkeeping than uniform grids.

Having chosen a discretized representation for the orbitals $\varphi_j(t_0)$ we have to approximate the time-ordered exponential in eq. (20). As a first simplification we drop the time-ordering over the time step Δt

$$\varphi_j(t+\Delta t) = \exp\left(-i\hat{H}_{KS}(t+\Delta t/2)\Delta t\right)\varphi_j(t), \qquad j=1,..,N\,. \tag{26}$$

Although this seems to be an ad hoc approximation it can be shown rigorously[17] that the discretization error introduced by this step is of the same order in Δt as the error introduced by the propagation schemes considered in this article. Only this fact justifies the omission of the time-ordering.

In the next two sections we review the Crank-Nicholson and split-operator schemes respectively and show how they have to be modified for the propagation of the Kohn-Sham equations.

3.1 Crank-Nicholson Propagator

Assuming a time-independent Hamiltonian the Crank-Nicholson (CN) scheme utilizes the so called Caley approximation to the time-evolution operator

$$\exp\left(-i\hat{H}\Delta t\right) = \frac{1-i\hat{H}\Delta t/2}{1+i\hat{H}\Delta t/2} + \mathcal{O}(\Delta t^3)\,. \tag{27}$$

This approximation is accurate up to second order in Δt, unconditionally stable and unitary. Inserting (27) in (26) results in an implicit approximation for the unknown orbital at $t+\Delta t$. In other words a set of linear equations has to be solved in each time step

$$[1+i\hat{H}\Delta t/2]\,\varphi_j(t+\Delta t) = [1-i\hat{H}\Delta t/2]\,\varphi_j(t)\,. \tag{28}$$

So far we have just considered the standard CN propagation. However, in a Kohn-Sham propagation the Hamiltonian is time-dependent. To account for this we can evaluate the Hamiltonian midway between two time steps as in (26)

$$[1+i\hat{H}_{KS}(t+\Delta t/2)\Delta t/2]\,\varphi_j(t+\Delta t) = [1-i\hat{H}_{KS}(t+\Delta t/2)\Delta t/2]\,\varphi_j(t)\,. \tag{29}$$

Now a further complication appears[18]. The Kohn-Sham Hamiltonian $\hat{H}_{KS}(t + \Delta t/2)$ depends via the Hartree and exchange-correlation potentials on the still unknown solutions $\varphi_j(t + \Delta t/2)$. To obtain an approximation for the Hamiltonian $\hat{H}_{KS}(t + \Delta t/2)$ we have to propagate with a two-step predictor-corrector approach. In the predictor step we use in (29) instead of $\hat{H}_{KS}(t + \Delta t/2)$ the retarded Hamiltonian $\hat{H}_{KS}(t)$

$$[1 + i\hat{H}_{KS}(t)\Delta t/2]\, \varphi'_j(t + \Delta t) = [1 - i\hat{H}_{KS}(t)\Delta t/2]\, \varphi_j(t) \,. \tag{30}$$

From the solution $\varphi'_j(t + \Delta t)$ the corresponding Hartree and exchange-correlation potentials are constructed, leading to the Hamiltonian $\hat{H}'_{KS}(t + \Delta t)$. In the corrector step we use the average

$$\hat{H}_{KS}(t + \Delta t/2) = \frac{\hat{H}'_{KS}(t + \Delta t) + \hat{H}_{KS}(t)}{2} \tag{31}$$

as approximation to $\hat{H}_{KS}(t + \Delta t/2)$. The numerical effort introduced by this predictor-corrector scheme is doubled compared to the ordinary CN propagation. Two linear systems have to be solved in each time step. This extra effort cannot be avoided since the approximation $\hat{H}_{KS}(t + \Delta t/2) \approx \hat{H}_{KS}(t)$ would cause a continuous decrease in energy due to the use of a somewhat retarded potential. In contrast the propagation with $\hat{H}_{KS}(t + \Delta t/2) \approx \hat{H}'_{KS}(t + \Delta t)$ causes an increase in energy due to the use of an advanced potential.

3.2 Split-Operator Scheme

The split-operator (SPO) technique exploits the fact that the total Hamiltonian can be split into two parts such that each part is diagonal in either configuration or momentum space. In general one finds for two non-commuting operators $\hat{A}$ and $\hat{B}$ the following splittings

$$\exp\left((\hat{A} + \hat{B})\lambda\right) = \exp\left(\hat{A}\lambda\right)\exp\left(\hat{B}\lambda\right) + \mathcal{O}(\lambda^2) \tag{32}$$

$$\exp\left((\hat{A} + \hat{B})\lambda\right) = \exp\left(\hat{A}\frac{\lambda}{2}\right)\exp\left(\hat{B}\lambda\right)\exp\left(\hat{A}\frac{\lambda}{2}\right) + \mathcal{O}(\lambda^3)\,. \tag{33}$$

This suggests the following approximations for the short-time propagator

$$\exp\left(-i\hat{H}\Delta t\right) = \exp\left(-i\hat{V}\Delta t\right)\exp\left(-i\hat{T}\Delta t\right) + \mathcal{O}(\Delta t^2) \tag{34}$$

and

$$\exp\left(-i\hat{H}\Delta t\right) = \exp\left(-i\hat{T}\frac{\Delta t}{2}\right)\exp\left(-i\hat{V}\Delta t\right)\exp\left(-i\hat{T}\frac{\Delta t}{2}\right) + \mathcal{O}(\Delta t^3)\,. \tag{35}$$

The propagation is now performed with the following steps

$$\varphi(\mathbf{r}, t) \xrightarrow{FT} \varphi(\mathbf{q}, t) \xrightarrow{\exp\left(-i\hat{T}\frac{\Delta t}{2}\right)} \varphi'(\mathbf{q}, t) \xrightarrow{FT} \varphi'(\mathbf{r}, t) \xrightarrow{\exp\left(-i\hat{V}\Delta t\right)} \varphi''(\mathbf{r}, t)$$

$$\xrightarrow{FT} \varphi''(\mathbf{q}, t) \xrightarrow{\exp\left(-i\hat{T}\frac{\Delta t}{2}\right)} \varphi'''(\mathbf{q}, t) \xrightarrow{FT} \varphi(\mathbf{r}, t + \Delta t)\,.$$

By switching between momentum and configuration space each of the exponentials can be evaluated in its diagonal representation causing only multiplications with phase factors.

The propagation with the SPO can be efficiently implemented by using Fast-Fourier Transforms. As in the case of the CN the SPO is unconditionally stable and unitary.

Let us now turn to a modification of the SPO scheme which allows for the propagation of the TDKS equations. Similar as in the last section we face the same problem. The time-dependent Hamiltonian has to be evaluated midway between two time steps and depends on the unknown solutions $\varphi_j(t + \Delta t/2)$. There is an elegant way to account for this lack of information in a SPO propagation. Consider again the short-time propagator

$$
\exp\left(-i\hat{H}_{KS}(t + \frac{\Delta t}{2})\Delta t\right) = \exp\left(-i\hat{T}\frac{\Delta t}{2}\right)\exp\left(-i\hat{V}_s(t + \frac{\Delta t}{2})\Delta t\right)\underbrace{\exp\left(-i\hat{T}\frac{\Delta t}{2}\right)}_{1.}
$$
$$
+\mathcal{O}(\Delta t^3) \tag{36}
$$

and think of the exponential (1.) in (36) as the first part of the low order splitting in (34) for half the time step

$$
\exp\left(-i\hat{H}_{KS}(t + \frac{\Delta t}{4})\frac{\Delta t}{2}\right) = \underbrace{\exp\left(-i\hat{V}_s(t + \frac{\Delta t}{4})\frac{\Delta t}{2}\right)}_{2.}\underbrace{\exp\left(-i\hat{T}\frac{\Delta t}{2}\right)}_{1.} +\mathcal{O}(\Delta t^2) . \tag{37}
$$

Since we only need the orbital densities to construct the Hartree and exchange-correlation potentials we have to evaluate the absolute value squared of the orbitals in configuration space

$$
\varphi_j(\mathbf{r}, t) \xrightarrow{FT} \varphi_j(\mathbf{q}, t) \xrightarrow{\exp\left(-i\hat{T}\frac{\Delta t}{2}\right)} \varphi_j'(\mathbf{q}, t) \xrightarrow{FT} \varphi_j'(\mathbf{r}, t) \xrightarrow{\exp\left(-i\hat{V}_s\frac{\Delta t}{2}\right)} \varphi_j''(\mathbf{r}, t) \longrightarrow |\varphi_j''(\mathbf{r}, t)|^2
$$

$$
\varphi_j'(\mathbf{r}, t) \longrightarrow |\varphi_j'(\mathbf{r}, t)|^2 = |\varphi_j''(\mathbf{r}, t)|^2 .
$$

Because the second exponential in (37) constitutes just a phase in configuration space it cancels when evaluating the absolute value. Therefore, it is sufficient to apply only the first exponential in (37). Also note that due to this cancellation the time argument of the Hamiltonian in (37) has no effect. Going back to (36) this is exactly what we have reached after the evaluation of the first exponential. Thus, we can construct a low-order approximation to $\varphi_j(t + \Delta t/2)$ or similarly to $\hat{V}(t + \Delta t/2)$ by calculating the orbital densities after the first exponential in (36). This approximation is then used in the second exponential in (36) for the unknown $\hat{V}(t + \Delta t/2)$.

Although we are reducing the order of the propagation error from $\mathcal{O}(\Delta t^3)$ to $\mathcal{O}(\Delta t^2)$ there is no extra effort required to obtain the Kohn-Sham potential midway between two time steps. The operator splitting generates the required information on the fly. This is in contrast to the adapted CN scheme of the last section where we have to double the numerical effort to be consistent in the time step. As a drawback of the SPO approach remains only the reduced order in the propagation error.

3.3 Strategies for Parallelization

One can think of several starting points for a parallelization of the Kohn-Sham time propagation using standard message-passing protocols such as the MPI standard. Depending

on the time-evolution algorithm this could be parallel FFT's in the case of the SPO or a distribution of the numerical grid over the available nodes in the case of a CN propagation. However, in both cases the implementation has to be done with great care. Grid boundaries have to be communicated between the nodes and a high information traffic is caused automatically. In contrast, the simplest and at the same time most efficient parallelization can be achieved by a distribution of the orbitals. Each node is assigned a fixed number of orbitals. The node is then computing the time evolution of the orbitals and is evaluating the partial orbital densities. In each time step the total density has to be evaluated only once from the partial densities and sent back to the nodes in order to calculate the effective single-particle potential. This approach reduces the communication traffic between the nodes to a minimum. Running such a parallelization on a cluster of modern workstations or PC's elapses on the order of 5 min per node for a time step of a single orbital. The traffic caused by the evaluation and forwarding of the total density requires on the other hand only a fraction of a second. Considering this ratio of traffic and computational load it is already sufficient to connect the nodes with a cheap 100 Mbit LAN. A further argument for this approach is the simplicity of the implementation. It took only 12 MPI commands in a code with more than 10.000 lines. This simplifies the debugging of such a code considerably.

4   Examples for the Solution of the TDKS Equations

For a given initial state the Runge-Gross theorem ensures a one-to-one mapping between time-dependent densities and time-dependent potentials. Hence, any observable of a time-dependent electronic system is a functional of the time-dependent density and the corresponding initial state. For most observables it is difficult to write down explicit approximations for the functional dependence on the time-dependent density and the initial state. However, in some cases the exact functional is known.

From a practical point of view any calculation within TDDFT is performed in two successive steps

(i) First the TDKS equations are solved for a given initial state and the time-dependent density is evaluated from the orbitals via eq (16).

(ii) Using the time-dependent density from step (i) and the initial state, the functional for the observable is evaluated.

Usually both steps involve approximations. To solve the TDKS equations some approximation for the exchange-correlation part of the effective single-particle potential has to be employed. Unless the exact functional for the observable is known, the second approximation enters in step (ii), where some approximate functional form for the density dependence of the observable of interest has to be assumed.

To illustrate the steps we review in the following sections two prototypical examples. First we discuss a density-functional treatment of high-harmonic generation (HHG). This constitutes a case where the exact functional is known, i.e. only approximations to $v_{xc}[\rho](\mathbf{r}, t)$ are required. The second example is the double-ionization of the Helium atom. In this case it is difficult to find explicit density functionals for the ion yield of singly and doubly ionized Helium, so that approximations in both steps (i),(ii) are involved.

4.1 High-Harmonic Generation

Even 35 years after the discovery of third-harmonic generation in a rare gas medium by New and Ward[19] the subject of high-harmonic generation is still a field of active research. The interest in HHG originates mainly from the perspectives for possible applications. The process is considered as a possible candidate for the generation of coherent VUV or soft X-ray pulsed sources.

For a density-functional treatment of HHG we follow the two-step procedure described above. Taking the optimized effective potential[16] as approximation for $v_{xc}[\rho](\mathbf{r}, t)$ the TDKS equations are solved for the Helium atom in a strong laser pulse

$$i\frac{\partial}{\partial t}\psi(\mathbf{r}, t) = \left(-\frac{\nabla^2}{2} - \frac{2}{r} + 2\int \frac{|\psi(\mathbf{r}', t)|^2}{|\mathbf{r} - \mathbf{r}'|} d^3 r + v_{xc}^{\mathrm{OEP}}(\mathbf{r}, t) + E_0 f(t) z \sin(\omega_0 t) \right) \psi(\mathbf{r}, t). \tag{38}$$

Here the laser field is treated in dipole approximation, has a frequency ω_0, a peak intensity E_0 and is taken to be linearly polarized in z-direction. The envelope $f(t)$ of the laser pulse describes a linear ramp over the first three cycles and is then held constant for the following 15 cycles.

In the second step of the calculation we have to evaluate the functionals for the observables of interest. In the case of harmonic spectra this can be done without any further approximation. Considering only the response of a single atom and neglecting propagation effects of the generated radiation in the medium, it can be shown[20] that the Fourier transform of the induced dipole moment

$$d(t) = \int z\, \rho(\mathbf{r}, t)\, d^3 r \tag{39}$$

is proportional to the experimentally observed harmonic distribution. Thus, the density functional for the harmonic spectra can be written down exactly

$$S[\rho](\omega) = |d(\omega)|^2 = \left| \int \exp(i\omega t) \left(\int z\, \rho(\mathbf{r}, t) d^3 r \right) dt \right|^2. \tag{40}$$

Note that the functional for harmonic spectra depends only on the density. Since the calculation is started in the ground state, the dependence on the initial state drops out. For this particular choice of initial state the initial Kohn-Sham orbitals can be obtained uniquely from the ground-state density by virtue of the traditional static Hohenberg-Kohn theorem. Together with the Kohn-Sham equation in (38) the functional $S[\rho](\omega)$ in (40) provides an efficient practical scheme for the systematic exploration of harmonic spectra. Repeating the computational procedure for different laser parameters ω_0 and E_0 or different envelopes $f(t)$ optimal conditions for the generation of high harmonics can be found. For example, by running different simulations, it turned out that two-color laser fields

$$E(t) = f(t)[E_0 \sin(\omega_0 t) + E_1 \sin(\omega_1 t + \delta)] \tag{41}$$

increase the efficiency of high-harmonic generation considerably. Typically the field strengths E_0 and E_1 are chosen to be of the same order and ω_1 is taken to be an integer multiple of ω_0. Possible phase shifts between the two fields are taken into account by the constant δ. In Fig. 1 we show the harmonic spectra for intensities $E_0 = E_1 = 0.01$ a.u., where the laser frequency ω_1 was adjusted to the second or third harmonic of the fundamental frequency $\omega_0 = 0.0740$ a.u. which corresponds to a wavelength of $\lambda = 616$ nm. The calculation shows that the harmonics from a two-color laser pulse can be more intense up to two orders of magnitude compared to a single color pulse[21]. Such results may be used to guide the experimental work in the search for coherent soft X-ray sources.
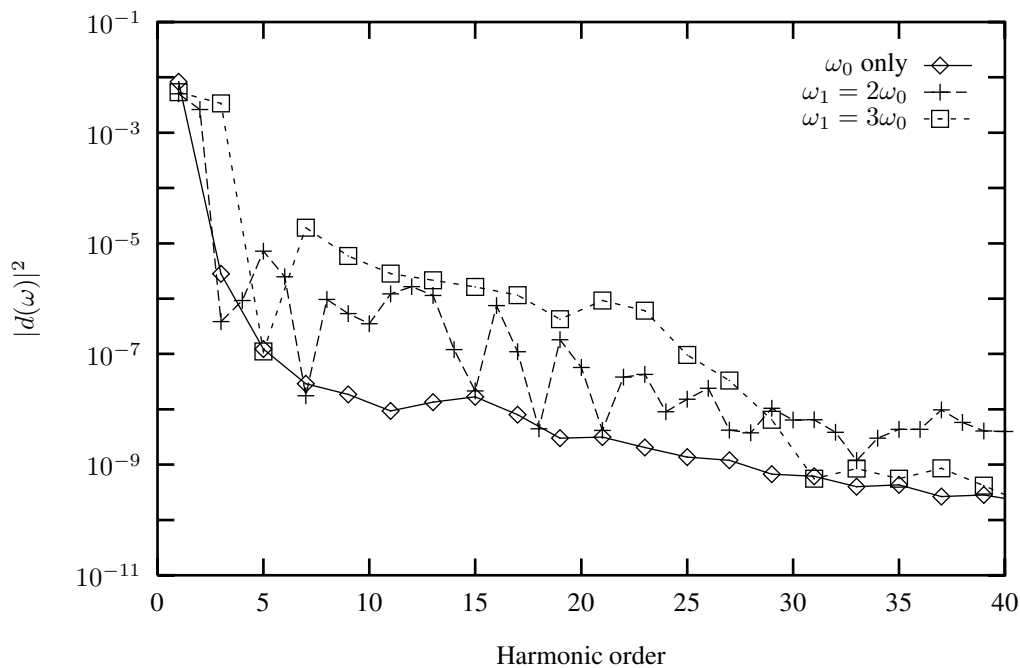

Figure 1. Harmonic spectra of helium calculated for one-color and two-color laser pulses with a total intensity of $I = 7.0 \cdot 10^{14}$ W/cm^2 respectively. The frequency of the second color has been adjusted to the second or third harmonic of the fundamental frequency $\omega_0 = 0.0740$ a.u. ($\lambda = 616$ nm).

4.2   Helium Double Ionization

When atoms or molecules are exposed to strong laser pulses there are three basic routes to analyze the laser-matter interaction. The first way is the observation of emitted harmonic light as discussed in the last section. The second route is to measure the kinetic energy and the angular distribution of the ionized electrons (photoelectrons) leaving the laser focus and the last possibility is to count the produced ions or to measure their momentum distribution. In this section we discuss a density-functional calculation of ion-yields for singly and doubly ionized atoms or molecules.

Considering laser pulses with a relatively long rise time it is well known[22] that the ionization dynamics is dominated by a "sequential" emission of electrons. With growing intensity the ionization yield of the singly ionized species grows according to the power law of the lowest non-vanishing order of perturbation theory. Only when a depletion of the neutral species starts to arise, an appreciable yield of doubly-ionized species can be detected. These properties of the ion yields can be described successfully with the single-active electron approximation[23, 24]: a stepwise scenario is assumed where the ionization occurs by a sequential emission of the electrons. The situation is different in the regime of ultra-short laser pulses. Experimentally it has been demonstrated in high-precision measurements[25] that double-ionization yields are up to six orders of magnitude larger than the rates expected in a sequential process. This is a clear manifestation of electron-electron correlation. Single-active electron calculations, by construction, will fail to describe the correlations involved in the ionization process. Time-dependent density-functional theory on the other hand is in principle capable to give the exact ionization yields, provided the exact functionals in the two-step procedure from above are known. For step (i) the familiar ALDA or TDOEP functionals can be used, so that only approximations for the ion-yields of singly P^{+1} and doubly P^{+2} ionized species have to be found. Using a geometrical concept that relies on the spatial partitioning of the wave function it is possible[26, 27] to find approximations for P^{+1} and P^{+2} in terms of the time-dependent density

$$P[\rho]^{+1}(t) = \int_A d^3r\,\rho(\mathbf{r},t) - \int_A d^3r_1 \int_A d^3r_2\,\rho(\mathbf{r}_1,t)\,\rho(\mathbf{r}_2,t)\,g[\rho](\mathbf{r}_1,\mathbf{r}_2,t)$$

$$P[\rho]^{+2}(t) = 1 - \int_A d^3r\,\rho(\mathbf{r},t) + \frac{1}{2}\int_A d^3r_1 \int_A d^3r_2\,\rho(\mathbf{r}_1,t)\,\rho(\mathbf{r}_2,t)\,g[\rho](\mathbf{r}_1,\mathbf{r}_2,t). \quad (42)$$

Here it was assumed that the Kohn-Sham propagation starts in the ground-state so that the dependence on the initial state drops out, similar to the case of harmonic spectra. In eq. (42), $g[\rho]$ denotes the pair-correlation function. This quantity is a density functional which, in practice, needs to be approximated. Following the same procedure as in section 4.1, the TDKS equation (38) is solved for the Helium atom in a strong laser pulse. From the resulting time-dependent density the functionals (42) are evaluated. Although this scheme provides a considerable improvement over sequential ionization yields it shows still a discrepancy of about two orders of magnitude when the results of the calculation are compared directly to experiment[26].

To test the relative importance of the two approximations involved in steps (i) and (ii), Lappas and van Leeuwen[28] have performed numerically exact time-propagations for a 1D soft core model of the Helium atom. Using the correlated Helium wave function, obtained in their simulation, exact reference values have been obtained for the ionization yields P^{+1} and P^{+2} of this model system. Since it is also possible to obtain the exact time-dependent density from the correlated Helium wave function, approximations involved in the first step (i) of the computational procedure can be circumvented. By evaluating the functionals for P^{+1} and P^{+2} (42) with the exact density the resulting approximate yields can be compared with the exact reference values and the performance of the functionals P^{+1} and P^{+2} can be tested directly. Lappas and van Leeuwen find that, although the double-ionization yields obtained in this way still show discrepancies, they reproduce the well known knee structure[25, 29] known from experiment. Since the knee cannot be obtained from the same

functional P^{+2} when approximate densities from TDOEP calculations are inserted, the approximations employed for the effective single particle potential $v_s[\rho]$ appear to have a bigger impact on the results.

References

1. *A comparison of different propagation schemes for the time-dependent Schrödinger equation*, C. Leforestier et al., J. Comput. Phys. **94**, 59-80 (1991).
2. *Quantum dynamics of the collinear (H, H_2) reaction*, E. A. McCullough, Jr. and R. E. Wyatt, J. Chem. Phys. **51**, 1253 (1969); **54**, 3592 (1971).
3. *Solution of the Schrödinger equation by a spectral method*, M. D. Feit, J. A. Fleck, Jr., and A. Steiger, J. Comput. Phys. **47**, 412-433 (1982).
4. *Inhomogeneous electron gas*, P. Hohenberg and W. Kohn, Phys. Rev. **136**, B 864 (1964).
5. *Self-consistent equations including exchange and correlation effects*, W. Kohn and L. J. Sham, Phys. Rev. **140**, A 1133 (1965).
6. *Density Functional Theory* , R. M. Dreizler and E. K. U. Gross, (Springer-Verlag, Berlin, 1990).
7. `http://www.gaussian.com`
8. `http://www.scm.com`
9. `http://www.fhi-berlin.mpg.de/th/fhimd/`
10. `http://www.wien2k.at`
11. `http://www.flapw.de`
12. `http://www.mpi-stuttgart.mpg.de/andersen/LMTODOC/LMTODOC.html`
13. `http://www.uam.es/departamentos/ciencias/fismateriac/siesta/`
14. *Density-functional theory for time-dependent systems*, E. Runge and E. K. U. Gross, Phys. Rev. Lett. **52**, 997 (1984).
15. *Density-functional theory of time-dependent phenomena*, E. K. U.Gross, J.F.Dobson and M.Petersilka in: *Topics in Current Chemistry: Density Functional Theory*. (ed.) R.F.Nalewajski, Springer, (1996).
16. *Time-dependent optimized effective potential*, C. A. Ullrich, U. J. Gossman, and E. K. U. Gross, Phys. Rev. Lett. **74**, 872 (1995).
17. *On the exponential form of time-displacement operators in quantum mechanics*, P. Pechukas and J. C. Light, J. Chem. Phys. **44**, 3897 (1966).
18. *One-dimensional nuclear dynamics in the time-dependent Hartree-Fock approximation* P. Bonche, S. Koonin, and J. W. Negele, Phys. Rev. C **13**, 1226 (1976).
19. *Optical third-harmonic generation in gases by a focused laser beam*, J. F. Ward and G. H. C. New, Phys. Rev. A **185**, 57 (1969).
20. *High-order harmonic generation: Simplified model and relevance of single-atom theories to experiment*, B. Sundaram, P. Milonni, Phys. Rev. A **41**, 6571 (1990).
21. *High harmonic generation in hydrogen and helium atoms subject to one- and two-color laser pulses*, S. Erhard and E. K. U. Gross, in: Multiphoton Processes 1996, P. Lambropoulus and H. Walther, ed(s), (IOP, 1997), p 37.
22. *Mechanisms for Multiple Ionization of Atoms by Strong Pulsed Lasers*, P. Lambropoulos, Phys. Rev. Lett. **55**, 2141 (1985).

23. *High-order harmonic generation from atoms and ions in the high intensity regime*, J. L. Krause, K. J. Schafer, and K. C. Kulander, Phys. Rev. Lett. **68**, 3535 (1992).

24. *Calculation of photoemission from atoms subject to intense laser fields*, J. L. Krause, K. J. Schafer, and K. C. Kulander, Phys. Rev. A **45**, 4998 (1992).

25. *Precision Measurement of Strong Field Double Ionization of Helium*, B. Walker, B. Sheehy, L. F. DiMauro, P. Agostini, K. J. Schafer, and K. C. Kulander, Phys. Rev. Lett. **73**, 1227 (1994).

26. *Strong-field double ionization of Helium, a density functional perspective*, M. Petersilka and E.K.U. Gross, Laser Physics **9**, 105 (1999).

27. *Ten topical questions in time-dependent density functional theory*, N. T. Maitra, K. Burke, H. Appel, E. K. U. Gross, and R. van Leeuwen, to appear in Reviews in Modern Quantum Chemistry: A Celebration of the Contributions of R. G. Parr, ed. K. D. Sen. (World Scientific,2001).

28. *Electron correlation effects in the double-ionization of He*, D. G. Lappas and R. van Leeuwen, J. Phys. B: At. Mol. Opt. Phys. **31**, L249-L256 (1998).

29. *Observation of nonsequential double ionization of helium with optical tunneling*, D. N. Fittinghof, P. R. Bolton, B. Chang and K. C. Kulander, Phys. Rev. Lett. **69**, 2642 (1992).